

# Direct dual layer spinning of aminosilica/Torlon<sup>®</sup> hollow fiber sorbents with a lumen layer for CO<sub>2</sub> separation by rapid temperature swing adsorption

Ying Labreche, Yanfang Fan, Ryan. P. Lively, Christopher W. Jones, William J. Koros

School of Chemical & Biomolecular Engineering, Georgia Institute of Technology, 311 Ferst Drive NW, Atlanta, Georgia 30332-0100

Correspondence to: W. Jones (E-mail: cjones@chbe.gatech.edu) and W. J. Koros (E-mail: wjk@chbe.gatech.edu)

**ABSTRACT:** The direct dual layer spinning of Torlon<sup>®</sup>/silica hollow fibers with a neat Torlon<sup>®</sup> lumen layer is reported here for the first time. The dual layer fibers containing a porous Torlon<sup>®</sup>/silica main structure and a dense, pure Torlon<sup>®</sup> polymer bore-side coating provide a simplified, scalable platform from which to construct hollow fiber amine sorbents for postcombustion CO<sub>2</sub> capture. After fiber spinning, an amine infusion process is applied to incorporate PEI into the silica pores. After combining dilute Neoprene treatment followed by poly(aramid)/PDMS treatment, a helium permeance of the fiber sorbents of 2 GPU with a He/N<sub>2</sub> selectivity of 7.4 is achieved. Ten of the optimized amine-containing hollow fibers are incorporated into a 22-inch long, 1/2 inch OD shell-and-tube module and the module is then exposed on the shell side to simulated flue gas with an inert tracer (14 mol % CO<sub>2</sub>, 72 mol % N<sub>2</sub>, 14 mol % He [at 100% R.H.]) at 1 atm and 35°C in a RTSA system for preliminary CO<sub>2</sub> sorption experiments. The fibers are found to have a breakthrough and equilibrium CO<sub>2</sub> capacity of 0.8 and 1.2 mmol/g- dry fiber sorbent, respectively. © 2015 Wiley Periodicals, Inc. *J. Appl. Polym. Sci.* 2015, 132, 41845.

**KEYWORDS:** adsorption; membranes; separation techniques; synthesis and processing

Received 4 September 2014; accepted 2 December 2014

DOI: 10.1002/app.41845

## INTRODUCTION

Climate change has motivated research activities to develop and improve processes for CO<sub>2</sub> capture. Cost-effective processes for CO<sub>2</sub> capture from flue gas streams of coal or gas-fired power plants are needed to enable post-combustion CO<sub>2</sub> capture to slow global climate change.<sup>1–3</sup> Among many process technology options used for CO<sub>2</sub> capture from flue gases, there is growing interest in adsorption processes. Such adsorption processes use solid sorbents to reversibly capture CO<sub>2</sub> from flue gas streams and present potential advantages over traditional liquid absorption processes. Specifically, the solid sorbents show reduced energy requirements for sorbent regeneration, greater sorption capacity, improved selectivity, and minimal equipment corrosion.<sup>4</sup> Adsorption on porous solids using pressure and/or temperature swing approaches is, therefore, an emerging alternative to reduce the costs associated with CO<sub>2</sub> capture.<sup>5,6</sup> The regeneration energy requirement for CO<sub>2</sub> capture using solid sorbents can be significantly reduced relative to traditional aqueous amine-based absorption processes, because of the absence of large amounts of water and elimination of

water and amine evaporation losses from the cycle. Moreover, the heat capacity of solid sorbents can be comparatively lower (about 1.6–2.4 J/°C·g) than those of an aqueous amine solvents (about 4 J/°C·g) when silica-based sorbents are used.<sup>7–11</sup>

Currently, most studies of solid sorbents have considered powder sorbents in lab-scale contactors such as fixed beds. Such beds cannot be scaled to the size needed for CO<sub>2</sub> capture from large electricity generating power plants and therefore looping bed configurations are being explored as alternatives.<sup>8,12,13</sup> However, the success of adsorption approaches for post-combustion CO<sub>2</sub> capture can greatly benefit from the synergistic development of sorbent materials that integrate with novel, practical, scalable contactors. Indeed, the sorbent/contacter combination should utilize materials with high adsorption capacities, high CO<sub>2</sub> selectivities, good durability, and allow for fast adsorption and desorption kinetics.<sup>6,7</sup> Many studies have examined CO<sub>2</sub> adsorption in porous silica sorbents containing amine groups.<sup>14–26</sup> While amine sorbents offer many of the needed characteristics described above, as chemisorbents, they would benefit from being deployed in a contactor whereby the heat of

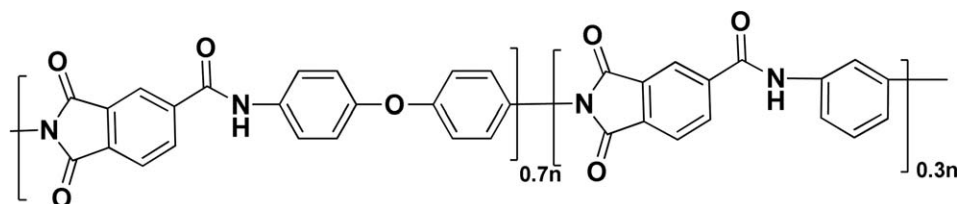


**Figure 1.** Structure of Torlon® 4000T, the poly(amide-imide) used in this article.

adsorption could be captured and heat-integrated into the overall capture process and/or power plant. To this end, we have worked for the past two years to evaluate the integration of supported amine adsorbents in novel polymeric hollow fiber contactors where such heat integration is possible.<sup>27–31</sup>

Polymer/oxide hollow fiber sorbents for rapid thermal swing adsorption (RTSA) of CO<sub>2</sub> from a dry simulated flue gas were first reported<sup>32</sup> in 2009 in a proof of concept study designed to evaluate the RTSA process approach. CA hollow fiber sorbents containing zeolite 13X as the CO<sub>2</sub> sorbent were spun to create fiber sorbents for CO<sub>2</sub> capture from dry CO<sub>2</sub> streams. In 2013, this work was extended using amine-loaded cellulose acetate (CA) polymer/silica hollow fiber sorbents by utilizing a post-fiber spinning amine infusion technique, which was demonstrated to apply to both PEI-impregnated (class 1)<sup>27</sup> and aminosilane-grafted (class 2) amine sorbents.<sup>28</sup> These first generation sorbents were shown to have intermediate breakthrough and pseudo-equilibrium CO<sub>2</sub> capacities, and the following year, the dynamic behavior of the aminosilica, PEI-based sorbents was explored.<sup>29</sup> More recently, we have extended the work to more robust poly(amide-imide) fibers based on the commercial polymer, Torlon®, while also significantly increasing the CO<sub>2</sub> sorption capacities via co-loading of glycerol with PEI in the pores of the silica particles.<sup>30</sup>

A critical piece of making the hollow fibers effective contactors is to install a low permeability lumen layer along the fiber bores, limiting or preventing transport of the heat transfer fluid from the bore side to the shell side of the contactor.<sup>33–38</sup> This enables the fibers to act as nanoscopic shell and tube heat exchangers. It has been demonstrated that the lumen side barrier layer can be created using a multistep polymer latex post-treatment, whereby a latex is flowed through the bore after fiber formation.<sup>30,36–38</sup> Although this approach can be effective, the array of materials currently suitable for use as lumen-layers is somewhat limited. From existing literature,<sup>36,39</sup> poly(vinylidene chloride) (PVDC) has adequately low permeabilities for many species; however, PVDC is thermally unstable in air above ca. 120°C because of dehydrochlorination at elevated temperatures.<sup>36</sup> Neoprene® (poly(chloroprene)), is an alternative material; however, it has higher permeabilities and requires a cross-linker to function as an effective barrier under practical operating conditions.<sup>30,36–38</sup> This cross-linking reaction can lead to cross-linked agglomerates that can plug the hollow fiber, making scale-up of this method complicated. This fact notwithstanding, our prior study showed that use of a Neoprene® latex provides a viable approach to form an effective lumen layer to create fiber sorbents suitable for CO<sub>2</sub> capture via RTSA.<sup>30</sup>

To avoid the above additional complexities, we report here a method to directly spin composite hollow fiber sorbents containing lumen layers via a simultaneous dual layer spinning with a sorbent-containing core dope plus a second inner pure polymer dope. The as-spun bore side polymer layer provides the barrier lumen layer, thereby removing the need for most of the post-spin processing with the concentrated polymer latex previously used to introduce the lumen layer. This approach also allows significant operational flexibility, e.g. the polymers on both sides of the fiber can be the same or different, depending on the fiber properties desired, so this approach represents a considerable step forward in preparing fiber sorbents.

This proof-of-concept work uses a poly(amide-imide) (PAI, Torlon®, Solvay Advanced Polymers®) as both the polymer matrix for the polymer/silica sorbent component and for the neat polymer lumen layer. The chemical structure of Torlon® is shown in Figure 1.<sup>30,40</sup> Torlon® is a good candidate for this application since it is a commercially available, chemically resistant, thermally stable, mechanically durable and has low vapor permeation properties.<sup>40,41</sup> Also, PAI polymers have been shown to allow high inorganic loadings for making composite fibers, with the oxide particles being homogeneously dispersible in the mixed-matrix type porous sorbent material.<sup>30,41,42</sup>

To achieve a high density, thick-walled lumen layer inside the hollow fiber, the traditional membrane hollow fiber bore fluid that is responsible for creating the fiber bore required modification. Specifically, a minimally invasive nonsolvent, poly(ethylene glycol) (PEG), was used as a component of the bore fluid in this work. To our knowledge, this is the first successful report of dual layer spinning of a hollow fiber with a bore-side lumen layer. The fibers have excellent barrier layer properties for both water and gases, so the method produces fibers with outstanding scope for use in this application as well as many others.

## EXPERIMENTAL

### Materials

PAI (Torlon®, Solvay Advanced Polymers®) and poly(vinylpyrrolidone) (PVP) (MW 55,000, Sigma-Aldrich) were used for formation of the hollow fiber sorbents. All polymers were dried in vacuum at 110°C for one day to remove moisture before use. *n*-Methyl-2-pyrrolidone (NMP) (Reagent Plus 99%, Sigma-Aldrich) was used as the solvent for the polymer-spinning dope. Methanol (MeOH) (99.8%, ACS Reagent, Sigma-Aldrich) and hexanes (ACS Reagent, >98.5%, Baker) were used for the solvent exchange portion of the fiber formation process, which occurs after spinning. Poly(ethyleneimine) (PEI) (MW 800, Sigma-Aldrich) was used as the amine source

**Table I.** Spinning Dope Composition (wt %)

	Fiber dope <sup>31</sup>	Lumen layer dope
PAI	14.01	27
PVP	3.92	-
Silica C803	14.01	-
NMP	59.93	66
Water	8.13	7

in the post-spinning amine infusion step, as discussed below. PEG (Mt 400, Sigma-Aldrich) was used as a component in the bore fluid. As noted above, PEG was selected as the nonsolvent for the extraction of NMP, because of its expected minimal inward diffusion during solvent extraction, plus its strong solubility for NMP and ability to withstand elevated spinning temperatures. Neoprene<sup>®</sup> or poly(chloroprene) was provided by DuPont Elastomers, Wilmington, DE, and a proprietary cross-linking reagent (TSR-633) developed specifically for Neoprene<sup>®</sup>, was obtained from Tiarco Chemical, Dalton, GA. Poly(dimethylsiloxane) (PDMS) (Sylgard<sup>®</sup> 184) was obtained from Dow Corning, and trimesoyl chloride (TMC) and diethyltoluene diamine (DETDA) were used as monomers for poly(aramid) in some of the work described. All solvents and nonsolvents were used as-received with no purification or modification. A commercial silica material, C803 (W.R. Grace, Lithonia, GA), was used as the amine support. C803 has a bulk density of 0.07–0.60 g/cm<sup>3</sup>, a particle size of 3.8 μm, an average pore diameter of 18.5–20 nm, a pore volume of 0.85 cm<sup>3</sup>/g and a BET surface area of 209 m<sup>2</sup>/g.

### Dual Layer Fiber Formation

A typical spinning dope to create a 50/50 silica/Torlon<sup>®</sup> sorbent layer contains the polymer PAI, sorbent particles, NMP (solvent), water (nonsolvent), and additives (PVP) (Table I).<sup>30</sup> The polymers and silica were dried at 110°C in a vacuum oven overnight prior to use.<sup>27</sup> Silica was added to 80% of the required NMP/water and sonicated using a 100 W sonication horn. The mixture was stirred and sonicated, and the bottle was warmed to about 40°C for 1 h (three cycles) to obtain a well-dispersed suspension. A “prime” dope was made from 20% polymer and 20% of the required NMP/water and was stirred for 48 hours on a roller. The dispersed silica mixture and prime dope were subsequently mixed together. This mixture was stirred and sonicated alternately for 1 h, and then the rest of polymer was added with mixing with a mechanical stirrer for 4 hours at 50°C to completely dissolve the polymer to form the final spin-ready dope.<sup>30</sup> The viscosity of the dope is too thick to measure with a Brookfield Digital Viscometer without heating a 50°C.

To form the lumen layer dope comprising PAI, NMP, and water, the PAI was simply dissolved in the solution of NMP and water. The dope was mixed for one week on a roller. The final polymer dope solution conditions chosen are listed in Table I. The ultimate lumen layer dope reflects the results of considerable optimization to enable proper function with the standard fiber dope reported in our earlier work.<sup>30</sup> The lumen layer dope has

a similar viscosity as the fiber dope so the two dopes interact well during the spinning step.

As noted above, dual layer fiber sorbents were spun with different bore fluids PEG/NMP/H<sub>2</sub>O and PEG, and these bore fluids were developed by extensive optimization. For efficiency, only the optimized composition is reported here. As before, the hollow fibers were formed using a non-solvent phase inversion technique commonly referred to as “dry-jet/wet-quench spinning”.<sup>43</sup> Spinning dopes were co-extruded with the optimized bore fluid through a triple orifice spinneret (Figure 2).

The nascent fiber was extruded into a nonsolvent (water) quench bath to induce phase separation and form a porous fiber with an intact, nonporous lumen layer. The fibers were removed from the take-up drum by clean cuts using a sharp blade and placed in a bath of deionized water for 1 week, wherein the water was changed every day, to remove residual solvent. The dual layer spinning system is shown schematically in Figure 3.

The dual layer spinneret dimensions<sup>44</sup> are shown in Figure 2 and the complete spinning conditions are given in Table II. After one week of daily water/NMP exchange, the fibers (approximately 75 g) were solvent exchanged by immersion in two successive aliquots (400 mL) of methanol for 20 min each followed by immersing in 400 mL 10% PEI solution of methanol.<sup>27</sup> Fibers were then removed from the bath and allowed to air dry in a fume hood for 1 h, then placed in a vacuum oven and dried for 2 h at 70°C.

### Hollow Fiber Post-Treatments

As is the case with most polymeric hollow fibers, selective layers may contain small defects that need post-treatments to seal. The primary post-treatment used in the current study was a simple, highly diluted Neoprene<sup>®</sup>/TSR-633 mixture in 50–75% water (Neoprene<sup>®</sup>:TSR-633 ratio of 89:11 by weight). Use of this dilute mixture is much simpler than the 85% solid latex used previously with single layer spinning and lumen layer installation entirely via postspinning treatment.<sup>30</sup> A 30-mL post-treatment solution was extruded through the 22 inch long, 10-fiber module bores followed by a 20 psig N<sub>2</sub> sweep stream for 5 s. Then the module was dried in air for 2 h and dried in a vacuum oven for 2 h at 70°C.

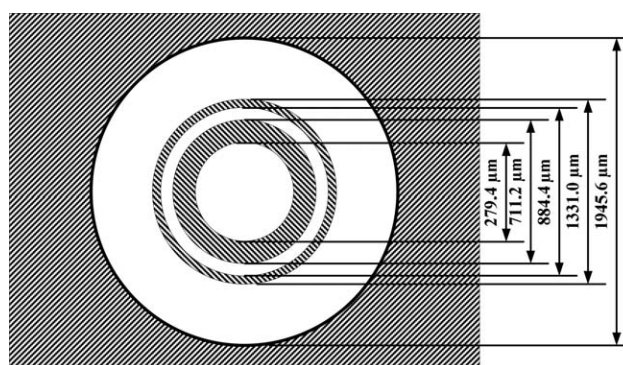


**Figure 2.** Annular dimensions of the custom-designed dual layer spinneret (striped parts are stainless steel and the white parts are empty for dopes and bore fluid to go through)

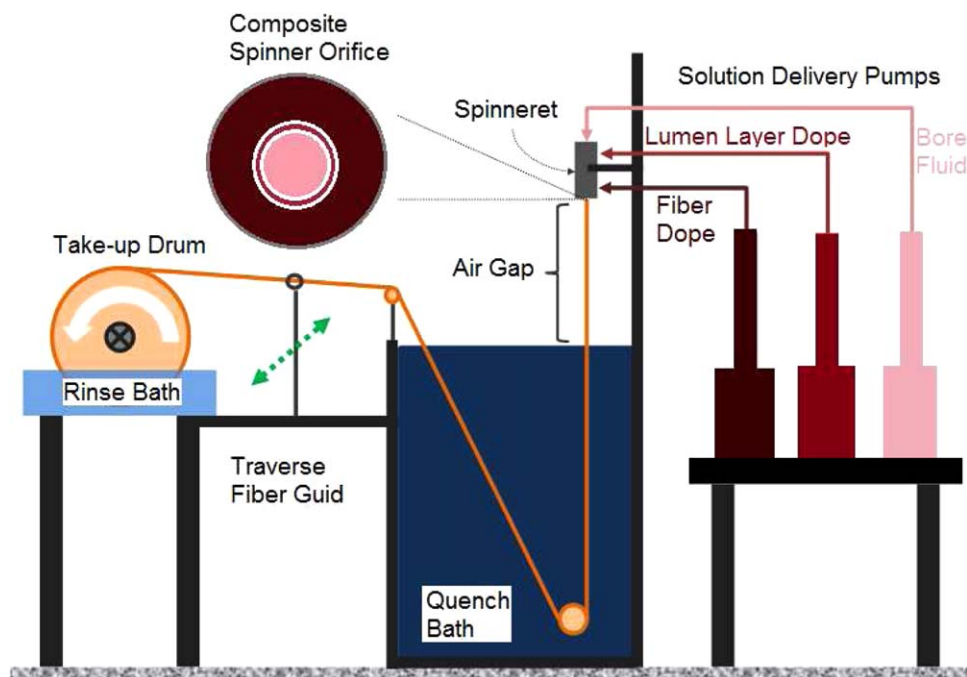


Figure 3. Dual layer spinning system. [Color figure can be viewed in the online issue, which is available at [wileyonlinelibrary.com](http://wileyonlinelibrary.com).]

The inner bore surface of the Neoprene<sup>®</sup> treated fibers was further coated with a dilute 2% PDMS and/or poly(aramid)/PDMS solution to seal fiber skin defects that might remain. This is similar to the standard post-treatment “caulking” used in conventional gas separation membranes to eliminate nanoscopic skin layer defects.<sup>45,46</sup> Specifically, for the treatment with only PDMS, 2 wt % PDMS in iso-octane was used, and after 30 min, the solution was drained and the residual iso-octane was removed from the fiber by degassing the fiber at 80°C for 2 h in a vacuum oven. The obtained fibers are referred to as PDMS-coated fibers. For the poly(aramid)/PDMS coating procedure,<sup>47,48</sup> the fibers were contacted with a solution of 0.2 wt % DETDA in iso-octane for 30 min and then the solution was drained. The fibers were then further contacted with a second solution of 0.2 wt % TMC and 2 wt % PDMS in iso-octane for 30 min followed by draining of the solution from the fibers. As the DETDA-impregnated fiber was brought into contact with

the TMC/PDMS solution, polycondensation occurred between the diamine (DETDA) and the crosslinker (TMC). As a result, a cross-linked poly(aramid) was formed within the network of PDMS on the fiber surface.<sup>49</sup> The residual iso-octane was then removed from the fiber by degassing the fiber at 80°C for 2 h in a vacuum oven. The obtained fibers are referred to as PDMS/poly(aramid)-coated fibers.

#### Materials Characterization

Scanning electron microscopy (SEM) imaging was done on a LEO 1530 field emission SEM (LEO Electron Microscopy, Cambridge, UK). The samples were sputter-coated with a 10–20 nm thick gold coating (Model P-S1, ISI, Mountain View, CA) before being transferred to the SEM for imaging. A thermogravimetric analyzer TGAQ500 (TA Instruments) was used for initial CO<sub>2</sub> adsorption characterization under dry conditions using a gas composed of 0.1 atm of CO<sub>2</sub> and 0.9 atm of He.

#### Fiber Module Characterization in a Simulated Flue Gas Flow System

Fibers were mounted in modules and adsorption/desorption characterization of the fiber modules was performed in a simulated flue gas flow using a multicomponent competitive adsorption system, described in detail in a previous work.<sup>29</sup> The fiber module was degassed under flowing N<sub>2</sub> at 90°C prior to CO<sub>2</sub> adsorption tests. Adsorption experiments were carried out by flowing a simulated flue gas (14 mol % CO<sub>2</sub>, 72 mol % N<sub>2</sub>, 14 mol % He (at 100% R.H.)) through the shell side of the temperature-controlled hollow fiber adsorbent module at 40 mL/min at 35°C or 55°C and 1 atm pressure. Helium was used as an inert tracer, N<sub>2</sub> acted as the carrier gas, and CO<sub>2</sub> was the adsorbate of interest. The concentration of CO<sub>2</sub> at the module outlet was transiently measured by mass spectrometry

Table II. Dual Layer Fiber Spinning Parameters

Spinning parameters	
Air gap height (cm)	3
Take-up rate (m/min)	5–20
Quench bath medium and temperature	H <sub>2</sub> O, 50°C
Spinneret temperature (°C)	50
Dual layer bore fluid composition	72.2/22.2/5.6, PEG/NMP/H <sub>2</sub> O and 100% PEG
Extrusion rate (mL/h)	Core: 800 and 600 mL/h, Bore: 120 and 80

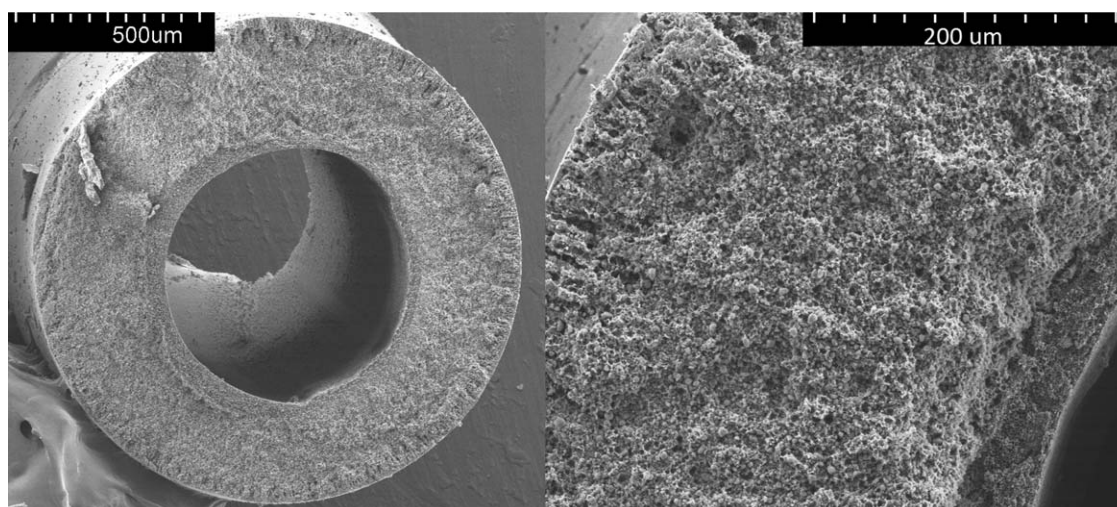


**Figure 4.** SEM images of the cross section of dual layer hollow fiber sorbents prepared with PEG/NMP as the bore fluid.

(ultrahigh vacuum Pfeiffer Vacuum QMS 200 Prisma Quadrupole Mass Spectrometer) from the start (0 s) until pseudo-equilibrium was reached (500 s). The total CO<sub>2</sub> uptake was calculated by integrating the area bounded by the CO<sub>2</sub> and He elution molar flow fronts (the He tracer accounts for the mean residence time within the system). The tests were carried out both with and without cooling water. The cooling water flow rate flowing through the bore was maintained at 70 mL/min.

## RESULTS AND DISCUSSION

### Dual Layer Torlon®/Silica/Torlon® Hollow Fiber Formation

To obtain a dense lumen layer on the inner surface of the hollow fiber, silica containing Torlon® PAI and pure Torlon® PAI dual layer fibers were spun. As described above, the traditional hollow fiber bore fluid, NMP/water,<sup>27</sup> was replaced by the minimally invasive nonsolvent mixture NMP/PEG/water and PEG. The PEG was used as a noninvasive nonsolvent coagulant.

When the bore fluid meets the lumen layer dope during the co-extrusion, the bore fluid PEG extracts the NMP from the lumen layer dope to the bore fluid. As a result, a thin, dense polymer layer is formed as an inner fiber skin layer.

A solution of PEG/NMP/H<sub>2</sub>O (72.2%/22.2%/5.6% by weight) was used as hollow fiber bore fluid. Extrusion rates were 800 mL/h for the core and 120 mL/h for the bore. SEM images of the dual layer hollow fiber sorbents, shown in Figure 4, demonstrate that the pure PAI lumen layer was formed successfully inside of the porous PAI/sorbent layer.

In this initial proof of concept study, it can be observed in some images that the centering of the lumen layer is not ideal and in some cases the two layers appear to be delaminated. The former issue can be addressed by improved spinneret alignment and experimental conditions in a future study. At this stage, it is unclear if the two layers in the fiber are delaminating under

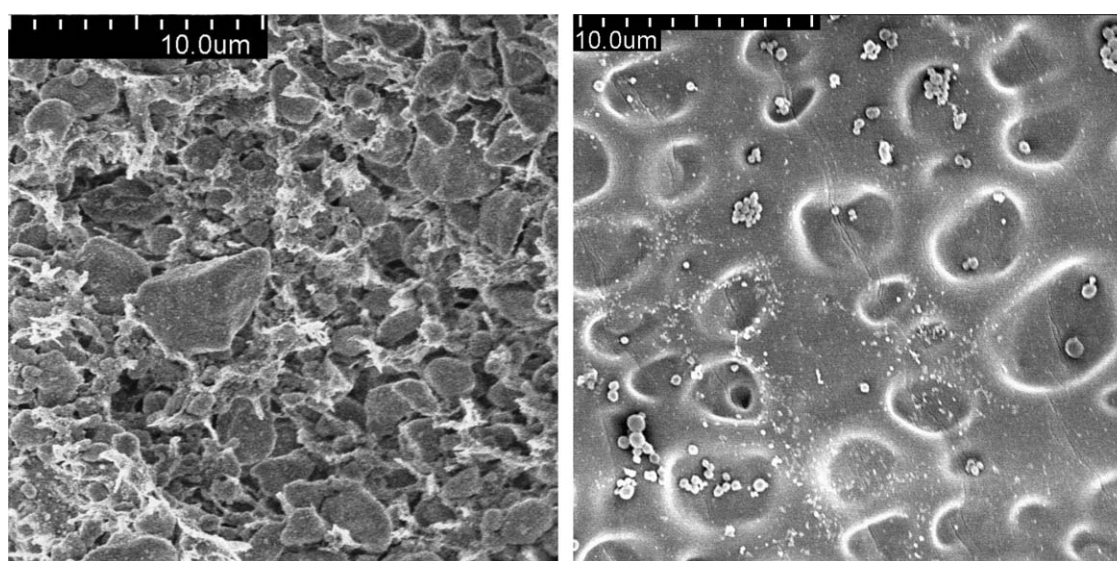


**Figure 5.** SEM images of the inner layer skin of a single layer fiber with silica particles (left) and a dual layer hollow fiber inner skin with no visible sorbents, as they are contained beneath the smooth skin layer.



**Figure 6.** Image of a flexible PAI/silica hollow fiber sorbent [minimum radius (Dime) 9 mm]. [Color figure can be viewed in the online issue, which is available at [wileyonlinelibrary.com](http://wileyonlinelibrary.com).]

normal handling or during fiber fracture for SEM imaging. While this sample preparation delamination indicates marginal interface strength under moderate temperature and nonshearing conditions, we expect the strength to be adequate for our applications, though some improvement may still be needed in future studies. The thickness of the inner layer can also be varied in future work as well. In regard to the CO<sub>2</sub> capacity per gram of fiber, the thinner the inner layer the better; however, with regard to spinning, a thinner layer makes the layer more defective. With improvements in the dual layer spinning technique, we anticipate that it will be possible to achieve dense wall thicknesses within the 5–10 μm range.

SEM images in Figure 5 show the inner wall skin of both single layer (bore fluid NMP/water 80 wt %/20 wt %) and dual layer hollow fiber sorbents (bore fluid PEG/NMP/H<sub>2</sub>O). The SEM images confirm differences in the fibers with and without the inner neat polymer layer. The silica particles can be seen at the surface of the single layer fiber, which has a rough, porous surface. The inner wall skin of the dual layer hollow fiber sorbent

**Table III.** He Permeances of Fiber Sorbents with and Without Lumen Layers at 35°C, 25 psig

Sample	He permeance, GPU <sup>a</sup>	α(He/N <sub>2</sub> )
Single layer Torlon <sup>®</sup> /silica/NMP/water	72,000 ± 300	1.7
Dual layer Torlon <sup>®</sup> /silica/NMP/PEG/water	3000 ± 50	2.0
Dual layer Torlon <sup>®</sup> /silica/PEG	1000 ± 30	2.0

<sup>a</sup>1 GPU = 1 × 10<sup>-6</sup> cm<sup>3</sup>(STP)/(cm<sup>2</sup>·s·cmHg).

has a polymer layer and is much smoother than the single layer fiber inner skin. The smoother inner layer will most likely make subsequent post-treatment more successful.

The flexibilities of single layer PAI/silica hollow fiber sorbents and CA/silica hollow fiber sorbents were evaluated by a bending test using coins with different diameters. The minimum curvature radius of the hollow fiber was defined by the smallest outer coin radius at which the fiber breaks.<sup>50</sup> The minimum bending radius (Dime, 9 mm) of PAI/silica hollow fiber sorbent is shown in Figure 6. The dual layer PAI/silica hollow fiber sorbent has the same minimum bending radius as the single layer PAI/silica hollow fiber sorbents, which may be expected since the outer layer materials are the same. CA/silica hollow fiber sorbents have a larger minimum bending radius (Quarter, 12 mm). It is clear that PAI/silica hollow fiber sorbents are more flexible with a smaller bending radius than the CA/silica hollow fiber sorbents. On the other hand, CA/silica hollow fiber sorbents are less flexible and more brittle because of the intrinsic properties of the CA polymer.

The array of fiber sorbents, including (i) single layer Torlon<sup>®</sup>/silica fibers prepared with NMR/water as the bore fluid, (ii) dual layer Torlon<sup>®</sup>/silica fibers prepared with NMP/PEG/water as the bore fluid, and (iii) dual layer Torlon<sup>®</sup>/silica fibers prepared using PEG as the bore fluid, were mounted in separate 12-in long modules to test their He permeances, which are indicative of the quality of the lumen layer installed in the fiber bores. Helium permeances through the single and dual layer hollow fiber sorbents were measured at 35°C and 25 psig. The results are listed in Table III. The goal for the lumen barrier layer was to achieve a He permeance as low as possible. The single layer Torlon<sup>®</sup>/silica fibers have 72,000 GPU He permeance<sup>37</sup> as high as Torlon<sup>®</sup>/silica fibers and CA/silica fibers (75,400 GPU).<sup>27</sup> The as-spun dual layer hollow fiber sorbents had lower He permeances of 3000 GPU (NMP/PEG/water as bore fluid) and 1000 GPU (PEG as bore fluid), compared with the single layer fiber (72,000 GPU with NMP/water as bore fluid). When pure PEG was used as the bore fluid, the resulting fibers had better permeation characteristics than the fibers made using the PEG solution (NMP/PEG/water) as the bore fluid. The dual layer fibers prepared using PEG as the bore fluid, with a He permeance of 1000 GPU, still warranted additional post-treatment to reduce the permeance further for practical operation in an RTSA process.

#### Post-Treatment of Partially Defective Dual Layer Fibers

For fibers that had low He permeance in the as-spun form, but where the He permeance was not yet low enough for practical application in an RTSA format, an additional diluted Neoprene<sup>®</sup> treatment was applied. Since the dual layer hollow fiber sorbents had smoother inner walls and lower He permeance than the single layer fibers, the Neoprene<sup>®</sup> treatment process step was much simpler than in previous work whereby application of a Neoprene<sup>®</sup> post-treatment was the sole method used to introduce a lumen layer.<sup>27</sup> The Neoprene<sup>®</sup> solution concentrations for the post-treatment step were optimized and the resulting fibers were compared to fibers treated with other post-

**Table IV.** He Permeances (35°C, 25 psig) of Fiber Sorbents with and Without Lumen Layers Prepared via Various Methods

Sample	He (GPU)	$\alpha(\text{He}/\text{N}_2)$
Dual layer fiber	1000 ± 50	2.0
Dual layer fiber/30 wt % Neoprene®	200 ± 20	2.0
Dual layer fiber/50 wt % Neoprene®	50 ± 5	2.0
Dual layer fiber/25 wt % Neoprene®, twice	6.9 ± 0.14	2.5
Dual layer fiber/25 wt % Neoprene®, twice +PDMS	3.3 ± 0.2	4.2
Dual layer fiber/25 wt % Neoprene®, twice+ poly(aramid) in PDMS	2.1 ± 0.14	7.4
Neat Torlon® fiber <sup>38</sup>	134	2.2
Neat Torlon® fiber/85% Neoprene® <sup>38</sup>	1.6 ± 0.2	4.8 ± 1.7

treatment approaches, specifically PDMS and PDMS/Poly(aramid) treatments, as shown in Table IV.

Among the Neoprene® post-treated fibers, fibers coated twice with 25% Neoprene® solutions gave the best permeance reduction without resorting to treatments with additional reagents, whereby the He permeation rate was reduced to ~7 GPU and the He/N<sub>2</sub> permeation ratio was 2.5.

The application of two coating treatments was convenient since both fiber ends must be coated to avoid end cap bypass.<sup>36</sup> To assess how low the He permeance could be reduced and to prevent as completely as possible water permeation from the bore to the shell when the fibers were being operated in RTSA mode, the fiber bores were further treated with a PDMS solution. In this case, the He permeation was reduced to 3 GPU and He/N<sub>2</sub> selectivity increased to 4. As desired, the lumen layer substantially decreased the He permeance of the PAI/silica/PEI hollow fiber sorbent, with an increase in the He/N<sub>2</sub> selectivity beyond the Knudsen diffusion limit of 2.65. Exceeding the Knudsen limit<sup>51</sup> means that a functional polymer layer lumen was created. It suggests that additional pinholes were effectively sealed by this treatment. To further reduce the permeance, the Neoprene® treated fibers were treated with a poly(aramid)/PDMS solution. Poly(aramid)s have been used as membrane coating materials in several studies,<sup>47,48</sup> where it was suggested that the monomers were compact enough to diffuse into and polymerize inside ultra-small defects, providing small interstitial seals that typically have not been achieved by bulkier PDMS-only treatments. After the fibers were coated with PDMS/poly(aramid), the He/N<sub>2</sub> selectivity was dramatically enhanced from 4 to 7.7. This suggests that poly(aramid) treatment was indeed more effective than PDMS alone to seal defects in the fibers. The reduced permeance of the PDMS/poly(aramid)-coated fibers (Table IV) indicates that the particular poly(aramid) used (based on DETDA and TMC) added substantial mass transfer

resistance to gas permeation. However, despite the progressive improvement in performance, it appears that simply dual Neoprene® treated fibers or even perhaps the singly Neoprene® treated fibers may be adequate for practical use of the fibers in RTSA mode. The simplicity of these treatments makes them potentially practical for scale-up in large-scale applications such as postcombustion CO<sub>2</sub> capture. Table IV combines literature data on neat Torlon hollow fibers and neat Torlon® fibers coated with 85% Neoprene<sup>37</sup> in the last two rows for comparison with the new fibers developed here. The best fiber developed here has a similar He permeance but higher He/N<sub>2</sub> selectivity fiber treated only with 85% Neoprene®.<sup>38</sup>

After testing the He permeances of the fibers, the water permeation rates through the lumen layer were tested using the RTSA system with N<sub>2</sub> flowing on shell side at 1 atm and cooling water in fiber bores flowing at 70 mL/min at 35°C. Figure 7 presents the water vapor content in shell side gas as a function of time for various modules with fibers post-treated in various ways. The fiber module treated by Neoprene® alone (25 wt % Neoprene®, twice) (a curve in Figure 7), still showed a measurable water permeation rate that elevated the water vapor content in the shell side carrier gas to 2 wt % after 10 minutes. Water permeation from the bore to the shell side has two key effects. On the negative side, water permeation results in water losses from a hypothetical closed, recirculating water system, and if the water is desorbed from the shell side during sorbent regeneration, extra energy will be required to achieve this desorption. On the positive side, the presence of moderate amounts of water have been shown to enhance CO<sub>2</sub> adsorption on amines by many authors,<sup>52,53</sup> and greater amine efficiency (moles CO<sub>2</sub> / moles amine) can be achieved under hydrated conditions using amine adsorbents. In practice, since the actual flue gas will tend to be saturated with water, low water losses may be anticipated via permeation across the lumen layer under practical conditions. In any case, when the fibers were further treated by PDMS (b curve in Figure 7), the water vapor permeation into the carrier gas was significantly reduced. Furthermore, the poly(aramid)/PDMS treatment further lowered the water

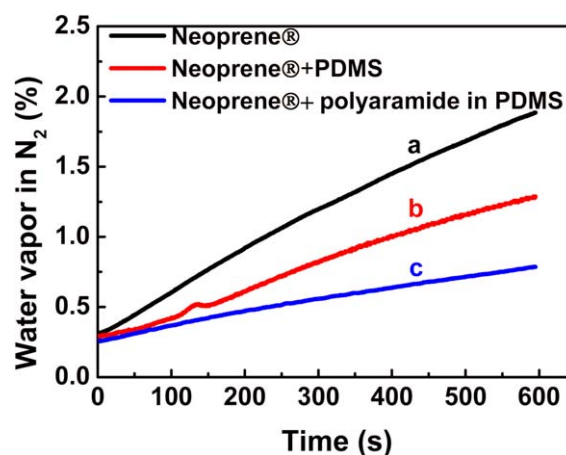


**Figure 7.** Water vapor content in shell side gas with flowing cooling water in fiber bores. [Color figure can be viewed in the online issue, which is available at [wileyonlinelibrary.com](http://wileyonlinelibrary.com).]

**Table V.** Single Layer Torlon<sup>®</sup>/Silica Neoprene<sup>®</sup> and Dual Layer Torlon<sup>®</sup>/Silica/PEI/Neoprene<sup>®</sup>/PDMS/Poly(Aramid) Hollow Fiber Breakthrough ( $q_b$ ) and Equilibrium ( $q_{pe}$ ) CO<sub>2</sub> Capacities Under Various Testing Conditions

Module test condition	CO <sub>2</sub> , $q_b$ , mmol/g-fiber	CO <sub>2</sub> , $q_{pe}$ , mmol/g-fiber
Single layer fibers without cooling water <sup>32</sup> , 35°C	0.82 ± 0.02	1.14 ± 0.02
Dual layer fibers without cooling water, 35°C	0.80 ± 0.02	1.17 ± 0.02
Dual layer fibers without cooling water, 55°C	0.89 ± 0.02	1.28 ± 0.02
Dual layer fibers with cooling water, 55°C	0.91 ± 0.02	1.2 ± 0.05

permeation, and this approach offered the best barrier properties of the various lumen layers tested here (c curve in Figure 7). The array of treatments summarized in Table V clearly demonstrates a variety of options for engineering lumen layers with various barrier properties.

Since the module containing dual layer fibers coated with Neoprene<sup>®</sup> + poly(aramid)/PDMS had the lowest water passage rate, this module was selected for further tests aimed at characterizing the CO<sub>2</sub> capture performance of the lumen-containing fibers.

#### Preliminary Assessment of Sorption Performance of Amine-Loaded Hollow Fiber Sorbent Modules Under Flowing Simulated Flue Gas

Ten dual layer amine-loaded sorbent fibers were assembled into a shell-and-tube module 22 inches long, and 1/2 inch in outer diameter and then exposed on the shell side at 1 atm and 55°C to simulated flue gas with an inert tracer [14 mol % CO<sub>2</sub>, 72 mol % N<sub>2</sub>, 14 mol % He (at 100% R.H.)]. The temperature of 55°C was chosen because this is the highest temperature at which the equipment can be operated with flowing bore side

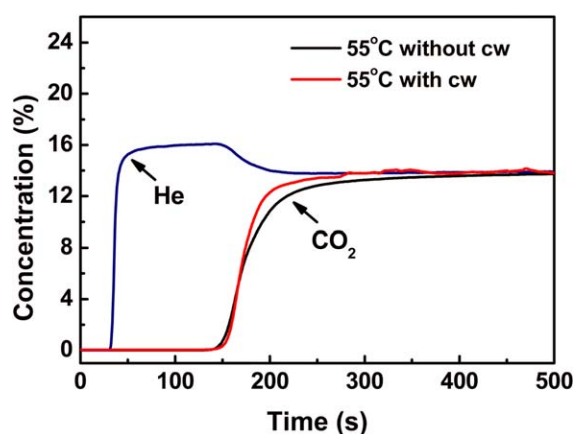


**Figure 8.** Comparison of breakthrough curves in dual layer Torlon<sup>®</sup>/silica/PEI/Neoprene<sup>®</sup>/PDMS/poly(aramid) hollow fibers without internal cooling water and with bore side cooling water at 55°C. [Color figure can be viewed in the online issue, which is available at [wileyonlinelibrary.com](http://wileyonlinelibrary.com).]

water. The Torlon<sup>®</sup>/silica/PEI/Neoprene<sup>®</sup>/PDMS/poly(aramid) hollow fiber breakthrough behavior is shown in Figure 8. As expected, a helium overshoot was observed as helium filled the void space of the fiber sorbent and then was subsequently displaced by the moving CO<sub>2</sub> front, thereby resulting in a slight increase in the helium concentration observed (a phenomenon known as “roll-up”).<sup>33,54,55</sup>

This dual layer Torlon<sup>®</sup>/silica hollow fiber sorbents have the same CO<sub>2</sub> capacities with the single layer Torlon<sup>®</sup>/silica hollow fiber sorbents. The CO<sub>2</sub> capacities of the fiber module with and without cooling water were measured at 55°C and the results are illustrated in Table V. The breakthrough curve profiles are compared in Figure 7. It can be seen that in both cases, CO<sub>2</sub> breaks through the module at the nearly same time. Both the breakthrough and pseudo-equilibrium CO<sub>2</sub> capacity ( $q_b$  and  $q_{pe}$ ) were similar under both conditions. Our previous work concluded that similar Torlon<sup>®</sup>/silica/PEI fibers without cooling water had the highest CO<sub>2</sub> capacity at 65°C.<sup>30</sup> Under such conditions, the uncooled module *in situ* temperature rise because of the exothermic adsorption was about 8–18°C,<sup>30</sup> making the CO<sub>2</sub> breakthrough capacity higher, because of enhanced the CO<sub>2</sub> diffusion rate in the PEI polymer at elevated temperatures. On the other hand, with cooling water in the bore side, the heat generated in the CO<sub>2</sub> adsorption process was rapidly transferred to the cooling water,<sup>29</sup> thereby reducing the CO<sub>2</sub> breakthrough capacity because of the lack of a temperature rise. However, the limited water passage through to the shell side from the bore side likely promoted a simultaneous increase of the adsorption capacity in the cooled fiber sorbent modules because of an adsorption mechanism effect discussed above, whereby the presence of water improves the amine efficiency.<sup>29,30</sup> These offsetting effects appear to lead to  $q_b$  and  $q_{pe}$  values for the fibers with cooling water that were very similar to the fibers run without cooling water. Thus, it is clear that the presence of cooling water in the bore side of the fibers along with some degree of water permeation from the bore to shell side can significantly impact the performance of the fiber sorbents. The ability to tailor a bore side lumen layer to control the water permeation rate therefore provides an additional measure of control of the overall adsorption/desorption process. A more detailed assessment of the dynamic permeation behavior of the dual layer sorbents will be reported separately.<sup>31</sup>

#### CONCLUSIONS

Direct dual layer fiber spinning was used to create composite fibers composed of a bore-side, PAI lumen layer coated on a PAI/silica/PEI hollow fiber structure. This direct spinning approach for lumen layer creation simplifies the fiber sorbent module lumen layer coating step required for use of the fibers in an RTSA system. Helium permeances of 2 GPU with a He/N<sub>2</sub> selectivity 7.4 were achieved at 35°C and 25 psig pressure after combining dilute Neoprene<sup>®</sup> treatment followed by poly(aramid)/PDMS treatment of the dual layer fibers. The fibers were then assembled into shell-and-tube modules and exposed on the shell side at 1 atm and 55°C to simulated flue gas with an inert tracer (14 mol % CO<sub>2</sub>, 72 mol % N<sub>2</sub>, 14 mol % He [at 100% R.H.]). The fibers were found to have a humid breakthrough CO<sub>2</sub> capacity of



0.9 mmol/g-fiber sorbent and the pseudo-equilibrium CO<sub>2</sub> uptake was 1.3 mmol/g-fiber sorbent, when operating in both cooled and uncooled mode (bore side, and no bore side cooling water flow, respectively). The dual layer fibers are thus demonstrated to be a promising platform from which to build composite polymer/aminosilica hollow fiber sorbents.

## ACKNOWLEDGMENTS

The authors acknowledge the DOE-NETL under contract DE-FE0007804 and GE for financial support. However, any opinions, findings, conclusions, or recommendations expressed herein are those of the author(s) and do not necessarily reflect the views of the DOE or GE.

## REFERENCES

1. Rackley, S. *Carbon Capture and Storage*; Butterworth-Heinemann: Cambridge, **2009**.
2. Aaron, D.; Tsouris, C. *Sep. Sci. Technol.* **2005**, *40*, 321.
3. Hedin, N.; Chen, L.; Laaksonen, A. *Nanoscale* **2010**, *2*, 1819.
4. Ma'mun, S.; Svendsen, H. F.; Hoff, K. A.; Juliussen, O. *Energ. Convers. Manage.* **2006**, *48*, 251.
5. Jones, C. W. *Annu. Rev. Chem. Biomol. Eng.* **2011**, *2*, 31.
6. Samanta, A.; Zhao, A. H.; Shimizu, G. K.; Sarkar, P.; Gupta, R. *Ind. Eng. Chem. Res.* **2012**, *51*, 1438.
7. Choi, S.; Drese, J. H.; Jones, C. W. *ChemSusChem.* **2009**, *2*, 796.
8. Bollini, P.; Didas, S. A.; Jones, C. W. *J. Mater. Chem.* **2011**, *21*, 15100.
9. Quang, D. V.; Rabindran, A. V.; Hadri, N. El.; Abu-Zahra, M. R. M. *Eur. Sci. J.* **2013**, *9*, 82.
10. Chiu, L.-F.; Liu, H.-F.; Li, M.-H. *J. Chem. Eng. Data* **1999**, *44*, 631.
11. Shih, T.-W.; Chen, Y.-J.; Li, M.-H. *Thermochim. Acta* **2002**, *389*, 33.
12. Bollini, P.; Brunelli, N. A.; Didas, S. A.; Jones, C. W. *Ind. Eng. Chem. Res.* **2012**, *51*, 15145.
13. Bollini, P.; Brunelli, N. A.; Didas, S. A.; Jones, C. W. *Ind. Eng. Chem. Res.* **2012**, *51*, 15153.
14. Hiyoshi, N.; Yogo, K.; Yashima, T. *Chem. Lett.* **2004**, *33*, 510.
15. Gray, M. L.; Soong, Y.; Champagne, K. J.; Pennline, H. W.; Baltrus, J.; Stevens, R. W.; Khatri, R.; Chuang, S. S. C. *Int. J. Env. Techn. Manag.* **2004**, *4*, 82.
16. Zheng, F.; Tran, D. N.; Busche, B. J.; Fryxell, G. E.; Addleman, R. S.; Zemanian, T. S.; Aardahl, C. L. *Ind. Eng. Chem. Res.* **2005**, *9*, 3099.
17. Franchi, R. S.; Harlick, P. J. E.; Sayari, A. *Ind. Eng. Chem. Res.* **2005**, *44*, 8007.
18. Xu, X. C.; Song, C. S.; Andresen, J. M.; Miller, B. G.; Scaroni, A. W. *Energy Fuels* **2002**, *16*, 1463.
19. Hicks, J. C.; Drese, J. H.; Fauth, D. J.; Gray, M. L.; Qi, G.; Jones, C. W. *J. Am. Chem. Soc.* **2008**, *130*, 2902.
20. Drese, J. H.; Choi, S.; Lively, R. P.; Koros, W. J.; Fauth, D. J.; Gray, M. M. L.; Jones, C. W. *Adv. Funct. Mater.* **2009**, *19*, 3821.
21. Huang, H. Y.; Yang, R. T.; Chinn, D.; Munson, C. L. *Ind. Eng. Chem. Res.* **2003**, *42*, 2427.
22. Belmabkhout, Y.; Serna-Guerrero, R.; Sayari, A. *Chem. Eng. Sci.* **2009**, *64*, 3721.
23. Xu, X. C.; Song, C. S.; Miller, B. G.; Scaroni, A. W. *Ind. Eng. Chem. Res.* **2005**, *44*, 8113.
24. Xu, X. C.; Song, C. S.; Miller, B. G.; Scaroni, A. W. *Fuel Process. Technol.* **2005**, *86*, 1457.
25. Xu, X. C.; Song, C. S.; Andresen, J. M.; Miller, B. G.; Scaroni, A. W. *Micropor. Mesopor. Mater.* **2003**, *62*, 29.
26. Xu, X. C.; Song, C. S.; Andresen, J. M.; Miller, B. G.; Scaroni, A. W. *Int. J. Environ. Technol. Manage.* **2004**, *4*, 32.
27. Labreche, Y.; Lively, R. P.; Rezaei, F.; Chen, G.; Jones, C. W.; Koros, W. J. *Chem. Eng. J.* **2013**, *219*, 166.
28. Rezaei, F.; Lively, R. P.; Labreche, Y.; Chen, G.; Fan, Y.; Koros, W. J.; Jones, C. W. *ACS Appl. Mater. Interfaces* **2013**, *5*, 3921.
29. Fan, Y.; Lively, R. P.; Labreche, Y.; Rezaei, F.; Koros, W. J.; Jones, C. W. *Int. J. Greenhouse Gas Control* **2014**, *21*, 61.
30. Labreche, Y.; Fan, Y.; Rezaei, F.; Lively, R. P.; Jones, C. W.; Koros, W. J. *ACS Appl. Mater. Interfaces* **2014**, *6*, 19336.
31. Fan, Y.; Labreche, Y.; Lively, R. P.; Jones, C. W.; Koros, W. J. *AIChE J* **2014**, *60*, 3878.
32. Lively, R. P.; Chance, R. R.; Kelley, B. T.; Deckman, H. W.; Drese, J. H.; Jones, C. W.; Koros, W. J. *Ind. Eng. Chem. Res.* **2009**, *48*, 7314.
33. Lively, R. P.; Chance, R. R.; Koros, W. J. *Ind. Eng. Chem. Res.* **2010**, *49*, 7550.
34. Determan, M. D.; Hoysall, D. C.; Garimella, S. *Ind. Eng. Chem. Res.* **2011**, *51*, 495.
35. Lively, R. P. *Hollow fiber sorbents for post-combustion CO<sub>2</sub> capture*; Ph.D. Dissertation, Georgia Institute of Technology, Atlanta, GA, **2011**.
36. Lively, R. P.; Mysona, J. A.; Chance, R. R.; Koros, W. J. *ACS Appl. Mater. Interfaces* **2011**, *3*, 3568.
37. Lee, J. S.; Hillesheim, P. C.; Huang, D.; Lively, R. P.; Hee, K.; Dai, O. S.; Koros, W. J. *Polymer* **2012**, *53*, 5906.
38. Li, F. S.; Lively, R. P.; Lee, J. S.; Koros, W. J. *Ind. Eng. Chem. Res.* **2013**, *52*, 8928.
39. Bicerano, J.; Burmester, A. F.; Delassus, P. T.; Wessling, R. A. *Transport of penetrant molecules through copolymers of vinylidene chloride and vinyl chloride, Barrier Polymers and Structures*, ACS Symposium Series 423, Ed by W. J. Koros, ACS, Washington, DC, **1990**.
40. Robertson, G. P.; Guiver, M. D.; Yoshikawa, M.; Brownstein, S. *Polymer* **2004**, *45*, 1111.
41. Wang, Y.; Jiang, L.; Matsuura, T.; Chung, T. S.; Goha, S. H. *J. Membr. Sci.* **2008**, *318*, 217.
42. Fritsch, D.; Peinemann, K. V. *J. Membr. Sci.* **1995**, *99*, 29.
43. Pesek, S. C.; Koros, W. J. *J. Membr. Sci.* **1994**, *88*, 1.

44. Wickramanayake, W. M. S.; Lively, R. P.; Polizzotti, R. S.; Chance, R. R.; Koros, W. J. *J. Appl. Polym. Sci.* **2011**, *121*, 2835.
45. Henis, J. M. S.; Tripodi, M. K. *Science* **1983**, *220*, 11.
46. Henis, J. M. S.; Tripodi, M. K. *Sep. Sci. Technol.* **1980**, *15*, 1059.
47. Ekiner, O. M.; Hayes, R. A.; Manos, P. Reactive post treatment for gas separation membrane. US Patent 5091216, **1992**.
48. Zhang, C.; Zhang, K.; Xu, L.; Labreche, Y.; Kraftschik, B.; Koros, W. J. *AIChE J.* **2014**, *60*, 2626.
49. Furuzono, T.; Yashima, E.; Kishida, A.; Maruyama, I.; Matsumoto, T.; Akashi, M. *J. Biomat. Sci. Polym. E* **1994**, *5*, 89.
50. Yoshimune, M.; Haraya, K. *Sep. Purif. Technol.* **2010**, *75*, 193.
51. Berg, van den, G. B.; Smolders, C. A. *J. Membr. Sci.* **1992**, *73*, 103.
52. Chang, A. C. C.; Chuang, S. S. C.; Gray, M.; Soong, Y. *Energy Fuels* **2003**, *17*, 468.
53. Danckwerts, P. V. *Chem. Eng. Sci.* **1979**, *34*, 443.
54. Li, G.; Xiao, P.; Xu, D.; Webley, P. A. *Chem. Eng. Sci.* **2011**, *66*, 1825.
55. Lively, R. P.; Chance, R. R.; Mysona, J. A.; Babu, V. P.; Deckman, H. W.; Leta, D. P.; Thomann, H.; Koros, W. J. *Int. J. Greenhouse Gas Control* **2012**, *10*, 285.